AD NUMBER

AD296036

NEW LIMITATION CHANGE

TO

Approved for public release, distribution unlimited

FROM

Distribution authorized to U.S. Gov't. agencies and their contractors; Administrative/Operational use; 31 Oct 1962. Other requests shall be referred to Army Engineer Research and Development Labs, Fort Belvoir, VA.

AUTHORITY

AEC ltr, 19 Apr 1966

AD 296 036

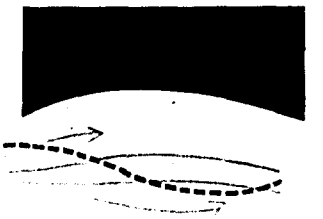

RELATIONSHIPS BETWEEN TROPICAL PRECIPITATION AND KINEMATIC CLOUD MODELS

REPORT NO. 2

Contract No. DA - 36-039 SC 89099

DA Project No. 3A 99-27-005

Second Quarterly Progress Report

1 August 1962 - 31 October 1962

Sponsored by U.S. Army Electronics Research and Development Laboratory
Fort Monmouth, New Jersey

THE TRAVELERS RESEARCH CENTER INC.

RELATIONSHIPS BETWEEN TROPICAL PRECIPITATION AND KINEMATIC CLOUD MODELS

Report No. 2

Contract DA-36-039 SC 89099

DA Project 3A 99-27-005

Second Quarterly Progress Report

1 August 1962–31 October 1962

OBJECT

The object of this research is to study relationships between tropical precipitation and the associated circulations of water vapor and condensate.

Prepared by: Edwin Kessler, III
Pieter J. Feteris
Edward A. Newburg

THE TRAVELERS RESEARCH CENTER, INC.
650 Main Street
Hartford 3, Connecticut

TABLE OF CONTENTS

PURPOSE

The purpose of the project is to increase understanding of the roles of cloud conversion, accretion, evaporation, and entrainment processes in shaping the distributions of water vapor, cloud, and precipitation associated with tropical circulations.

ABSTRACT

A system of conservation equations embodying conversion of cloud to precipitation and cloud collection by precipitation are examined. The steady precipitation rate at the base of a model updraft column is shown to be a maximum when cloud conversion and collection are complete above the level of nondivergence and zero below that level. The decrease of saturation vapor density with height, characteristic of the atmosphere, implies that for any cloud-water content, there is a level (compensation level) above which the cloud density decreases with ascending motion, and conversely. For a particular choice of the magnitude of cloud collection, the precipitation rate at the ground and its time of onset is rather insensitive to the rate of cloud conversion. The efficiency of precipitation production at the earth's surface by transient disturbances in a saturated model atmosphere decreases with increasing speed of the updraft. Paths for further study of the role of cloud conversion and cloud collection processes for the initiation of precipitation are indicated. The difference between the horizontal speed of raindrops and the horizontal wind speed is almost always less than 1% of representative horizontal winds.

PUBLICATIONS, LECTURES, REPORTS, AND CONFERENCES

A paper entitled "Relationships Between Tropical Precipitation and Kinematic Cloud Models" was submitted to and accepted by the Program Committee for the 43rd Annual Meeting of the American Meteorological Society (New York City). This paper is scheduled for presentation on January 21, 1963.

On September 4, Drs. Kessler and Newburg and Mr. Feteris visited the U.S. Army Electronics Research and Development Laboratory and discussed various matters pertaining to the work in progress and future plans.

1.0 FACTUAL DATA

1.1 A Model of the Bulk Effects of recipitation-Cloud Interactions

The derivation of continuity equations for cloud and precipitation and exposition of methods for solving them are outlined in Sections 1.4ff of the first report of this contract, and background details are in the literature [7, 8, 9]. In their general forms, the equations considered are

$$\frac{\partial M}{\partial t} = - u \frac{\partial M}{\partial x} - v \frac{\partial M}{\partial y} - w \frac{\partial M}{\partial z} - \frac{\partial}{\partial z} MV + Mw \frac{\partial \ln \rho}{\partial z} + \text{cloud conversion} + \text{cloud collection} - \text{evaporation} \tag{1}$$

and

$$\frac{\partial m}{\partial t} = - u \frac{\partial m}{\partial x} - v \frac{\partial m}{\partial y} - w \frac{\partial m}{\partial z} + wG + mw \frac{\partial \ln \rho}{\partial z} - \text{cloud conversion} - \text{cloud collection} + \text{evaporation}. \tag{2}$$

Equations (1) and (2) incorporate the following continuity equation for air:

$$\frac{\partial u}{\partial x} + \frac{\partial v}{\partial y} + \frac{\partial w}{\partial z} + w \frac{\partial \ln \rho}{\partial z} = 0. \tag{3}$$

In Eq. (1), M (always ≥ 0) is the density of precipitation in grams per cubic meter and refers to that portion of the condensate which has an appreciable fall speed relative to the air. M is assumed to be distributed over an exponential population (Marshall-Palmer distribution [12]) of particle sizes. $V < 0$ is the terminal fall speed of the precipitation particle whose diameter D_0 divides the exponential distribution into parts of equal water content. The components of air motion in the x- and y- (horizontal) and z- (vertical) directions are given by u, v, and w respectively; ρ is the density of air; and t is time.

In Eq. (2), m is the cloud density plus the vapor density minus the saturation vapor density, and may be positive, negative, or zero. When m is positive, it represents the density of cloud, defined as condensate whose terminal fall speed is zero. When m is negative, it represents the amount by which the actual vapor density is less than saturation. G, a function of height, is called the generating function: $G = - \rho (dQ_s/dz)$, where Q_s is the saturation mixing ratio

of water vapor in air. The cloud-conversion, cloud-accretion, and evaporation terms are discussed in Report No. 1; they define, respectively, the spontaneous conversion of cloud to precipitation, the collection of cloud particles by precipitation, and the evaporation of precipitation. Because the model requires immediate evaporation of cloud in subsaturated air, evaporation of precipitation does not occur at the same time and place as cloud conversion and accretion.

Equations (1) and (2) relate local time changes of precipitation, cloud, and vapor, to transport, generation, and exchange processes. The first three terms on the right of both equations measure effects of advection by the wind. The term $\partial(Mv)/\partial z$ in Eq. (1) measures the vertical divergence of the mass flux of precipitation. This term does not appear in Eq. (2) because $V = 0$ for cloud. The terms in $w[(\partial \ln\rho)/\partial z]$ account for the compressibility of a horizontally uniform atmosphere.* Equations (1) and (2) can be solved for time-dependent fields of precipitation, cloud, and vapor when initial and boundary conditions with the wind field, the generating function, and the cloud physics terms are specified.

1.2 Idealized Steady-state Precipitation Rates from a Saturated Horizontally Uniform Updraft Column

At a shower core or near the center of a widespread precipitation area, the horizontal advection terms in Eqs. (1) and (2) vanish and the sum of the equations is

$$\frac{\partial (m+M)}{\partial t} = - w \frac{\partial (M+m)}{\partial z} - \frac{\partial}{\partial z} MV + wG + (m + M) \frac{\partial \ln\rho}{\partial z}. \qquad (4)$$

Consider the vertical integral of Eq. (4) in the steady case:

$$0 = - \int_0^H w \frac{\partial (m+M)}{\partial z} dz - \int_0^H \frac{\partial}{\partial z} MV \, dz + \int_0^H wG \, dz + \int_0^H (m+M) w \frac{\partial \ln\rho}{\partial z} dz. \qquad (5)$$

*When M, m, and G are in mixing ratio units, Eqs. (1) and (2) are the same except that $Mw[(\partial \ln\rho)/\partial z]$ in Eq. (1) becomes $-MV[(\partial \ln\rho)/\partial z]$, $mw[(\partial \ln\rho)/\partial z]$ is completely dropped from Eq. (2), and $G = -dQ_s/dz$.

The limits of integration are from the base, z = 0, to the top, z = H, of the updraft column. The second integral on the right is $(MV)_{z=H} - (MV)_{z=0}$; since M = 0 at the top of the updraft column, this is just the precipitation rate R_0 at the base of the updraft. R_0 can be taken as the precipitation rate at the ground without loss of generality. The third integral on the right is the condensation rate in a vertical column of unit cross section.

The first integral is studied by integration by parts. Note that

$$- w \frac{\partial (m+M)}{\partial z} = - \frac{\partial}{\partial z} [w (m + M)] + (m + M) \frac{\partial w}{\partial z}. \qquad (6)$$

The integral from z = 0 to z = H of the first term on the right of Eq. (6) vanishes because w is zero at the base and at the top of the updraft column. The divergence of the vertical wind in the second term on the right can be replaced by its equivalent in the equation of continuity for air, Eq. (3). Substitution from Eq. (3) into Eqs. (6) and (5), with the other simplifications noted above, gives

$$R_0 = \int_0^H wG \, dz - \int_0^H (m + M)\left(\frac{\partial u}{\partial x} + \frac{\partial v}{\partial y}\right) dz . \qquad (7)$$

Equation (7) is a reminder that the horizontal divergence of the wind is implicit even in the one-dimensional forms of Eqs. (1) and (2). The last term in Eq. (7) may be positive, negative, or zero, and is largely dependent on the magnitude and distribution of the ratio of precipitation fall speed to the updraft. Because horizontal convergence characterizes the lower part of an updraft column, and horizontal divergence the upper part, precipitation rates in excess of the condensation rate are favored by relatively large values of m and M below the level of no horizontal divergence. Equation (7) is the same whether the atmosphere is assumed to be compressible or incompressible. However, as shown elsewhere for the cloud-free model [7, Fig. 1] and for m in Section 1.3 of this report, the vertical distributions of M and m vary somewhat with the considerations of compressibility, and so must the effect of the divergence term in Eq. (7).

It is possible to treat certain simple distributions of cloud and precipitation by exact methods paralleling those described in the references. These cases are interesting as limiting forms associated with limiting values of the precipitation rate. They indicate how extreme modification of cloud-precipitation interactions could affect the spatial distributions of cloud and precipitation and the areal distribution of the precipitation rate at the ground.

Case 1. The cloud conversion term is identically zero. When the cloud conversion term is identically zero, M is zero throughout the depth of the updraft column, and, therefore, so must be the precipitation rate at the ground. In this case, manipulations like those used to derive Eq. (7) readily show that the terms on the right of Eq. (7) are equal and opposite in sign. In this case, condensate existing in the updraft column is removed by divergence aloft as rapidly as it is formed. The cloud either evaporates elsewhere in downdrafts or, after changing to precipitation, falls toward the ground at some place removed from the updraft core. The steady vertical distribution of cloud in an incompressible atmosphere is given by

$$m(z) = \int_0^z G \, dz \, . \qquad (8)$$

Figure 1, top, shows the steady vertical distribution of cloud for case 1 for constant and linear distributions of G in an incompressible atmosphere. As Eq. (8) shows, the cloud distributions are independent of the updraft distribution.

Case 2. The cloud conversion term is zero above the level of nondivergence; below this level cloud conversion and collection by precipitation proceed so rapidly that no cloud coexists with precipitation. In this case, the precipitation content is zero at the level of nondivergence and increases in the downward direction from there to the ground. Above the level of nondivergence, all condensation remains as cloud and is borne away by

horizontal divergence. The distribution of cloud above the level of nondivergence is given by an equation like (8). The distribution of precipitation below the level of nondivergence is given by

$$M(z) = \int_{H/2}^{z} \frac{wG}{w + V}\, dz. \tag{9}$$

Case 2 distributions of cloud and precipitation are shown in Fig. 1, center, for two ratios of precipitation fall speed to maximum updrafts and for two distributions of G in an incompressible atmosphere. The distributions of M are based on updrafts $w = [(4\, w_{max})/(H)](z - z^2/H)$ in this and following cases.

Case 3. The cloud conversion and collection terms are so large that all condensate appears immediately as precipitation of fall speed V. This is the cloudless case discussed in the references. For constant V, the steady surface precipitation rate at updraft cores always exceeds the vertically integrated condensation rate in a vertical column. As the ratio of precipitation fall speeds to updrafts declines toward unity, the core precipitation rate increases at the expense of the rates away from the core. On the other hand, when fall speeds are much larger than maximum updrafts, the core precipitation rate is only slightly larger than the vertically integrated condensation. Distributions of precipitation in this case are shown in Fig. 1, bottom, for two ratios of precipitation fall speed to maximum updrafts and for two distributions of G in an incompressible atmosphere.

Cases 4 and 5. Above the level of nondivergence, cloud conversion and collection proceed so rapidly that cloud is nonexistent; below the level of nondivergence, conversion and collection are zero, and at each height the cloud amount equals the amount of condensation in air lifted from

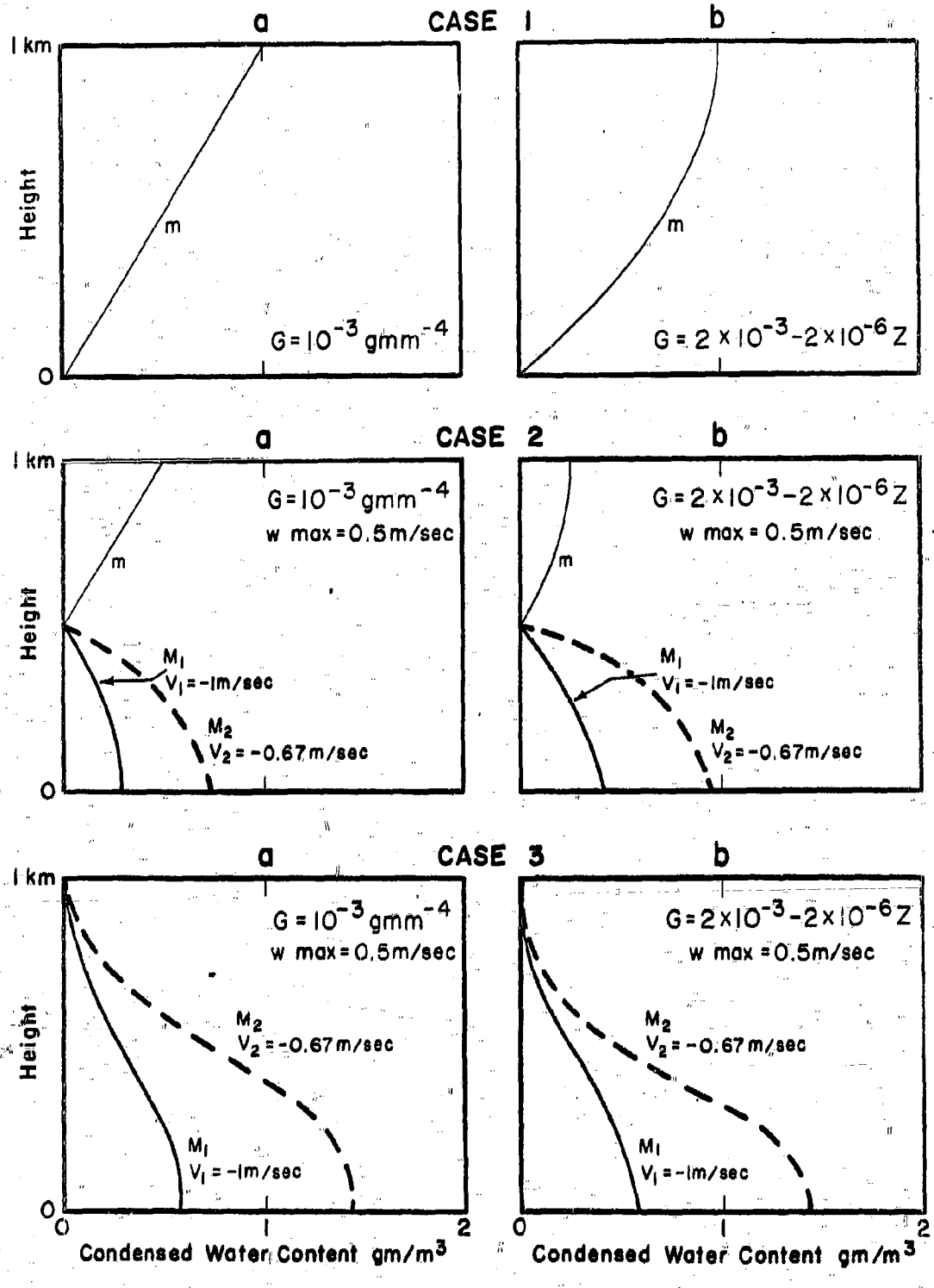

Fig. 1. Vertical profiles of cloud and precipitation.

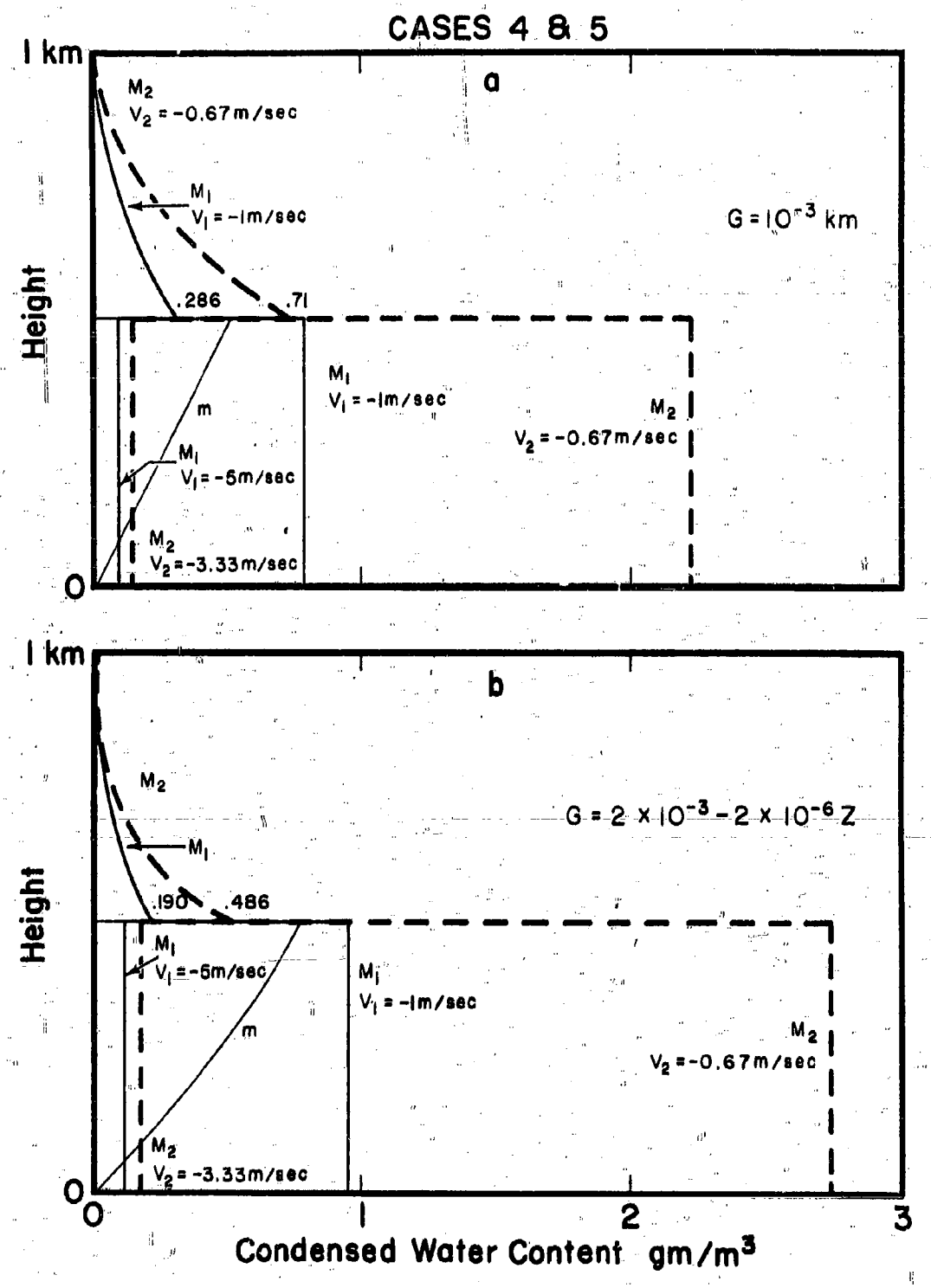

Fig. 2. Vertical profiles of precipitation and cloud.

Cloud and precipitation distributions in idealized one-dimensional cases*

Table 1

z	m_a	m_b	w	M	R	$wG_a dz$	$wG_b dz$
1	1.0	1.0	0	0	0	0	0
0.5	0.5	0.75	0.5	0	0	.17	.11
0	0	0	0	0	0	.33	.33

Table 2a

z	m	V_1	V_2	$w+V_1$	$w+V_2$	M_1	M_2	R_1	R_2
1	0.5	-	-	0	0	0	0	0	0
0.5	0	-	-	.5	0	0	0	0	0
0.5	0	-1	-.67	-.5	-.16	0	0	0	0
0	0	-1	-.67	-1	-.67	.29	.71	.29	.47

Table 2b

z	m	V_1	V_2	$w+V_1$	$w+V_2$	M_1	M_2	R_1	R_2
1	0.5	-	-	0	0	0	0	0	0
0.5	0	-	-	.5	0	0	0	0	0
0.5	0	-1	-.67	-.5	-.16	0	0	0	0
0	0	-1	-.67	-1	-.67	.38	.95	.38	.65

Table 3a

z	m	V_1	V_2	$w+V_1$	$w+V_2$	M_1	M_2	R_1	R_2
1	0	-1	-.67	-1	-.67	0	0	0	0
0.5	0	-1	-.67	-.5	-.17	.29	.71	.14	.12
0.5	0	-1	-.67	-.5	-.17	.29	.71	.14	.12
0	0	-1	-.67	-1	-.67	.57	1.42	.57	.95

Table 3b

z	m	V_1	V_2	$w+V_1$	$w+V_2$	M_1	M_2	R_1	R_2
H	0	-1	-.67	-1	-.67	0	0	0	0
0.5	0	-1	-.67	-.5	-.17	.19	.49	.10	.08
0.5	0	-1	-.67	-.5	-.17	.19	.49	.10	.08
0	0	-1	-.67	-1	-.67	.57	1.42	.57	.95

Table 4a

z	m	V_1	V_2	$w+V_1$	$w+V_2$	M_1	M_2	R_1	R_2
1	0	-1	-.67	-1	-.67	0	0	0	0
0.5	0	-1	-.67	-.5	-.17	.29	.71	.14	.12
0.5	.5	-1	-.67	-.5	-.17	.79	2.21	.39	.37
0	0	-1	-.67	-1	-.67	.79	2.21	.79	1.47

Table 4b

z	m	V_1	V_2	$w+V_1$	$w+V_2$	M_1	M_2	R_1	R_2
1	0	-1	-.67	-1	-.67	0	0	0	0
0.5	0	-1	-.67	-.5	-.17	.19	.49	.10	.08
0.5	.75	-1	-.67	-.5	-.17	.94	2.73	.47	.46
0	0	-1	-.67	-1	-.67	.94	2.73	.94	1.82

Table 5a

z	m	V_1	V_2	$w+V_1$	$w+V_2$	M_1	M_2	R_1	R_2
1	0	-1	-.67	-1	-.67	0	0	0	0
0.5	0	-1	-.67	-.5	-.17	.29	.71	.14	.12
0.5	.5	-5	-3.33	-4.5	-2.83	.09	.13	.39	.37
0	0	-5	-3.35	-5	-3.35	.09	.13	.44	.44

Table 5b

z	m	V_1	V_2	$w+V_1$	$w+V_2$	M_1	M_2	R_1	R_2
1	0	-1	-.67	-1	-.67	0	0	0	0
0.5	0	-1	-.67	-.5	-.17	.19	.49	.10	.08
0.5	.75	-5	-3.33	-4.5	-2.83	.10	.16	.47	.46
0	0	-5	-3.35	-5	-3.35	.10	.16	.52	.54

*These tables list the values of m and M at z = 0, z = 0.5 km and z = H = 1 km with updrafts $w = 2 \times 10^{-3} \times [z - 0^{-3}z^2]$. Tables 1, 2, and 3 refer to correspondingly numbered figures and cases discussed in the text. The values of w and $\int wGdz$ in Table 1 are the same for all the other tables. Tables 4 and 5 are included in Fig. 2 and refer to Case 4 discussed in the text. Tables 2a, 3a, 4a, 5a, refer to the generating function $G_a = 10^{-3}$ gm m^{-4}. Tables 2b, 3b, 4b, 5b, refer to the generating function $G_b = 4 \times 10^{-3} - 2 \times 10^{-6}z$. M_1 (gm m^{-3}) and R_1 (gm m^{-2} sec^{-1}) are the precipitation water content and rate in the case V_1 = -1m sec^{-1}. M_2 and R_2 apply to the case V_2 = -.67 m sec^{-1}. In tables 5a, and 5b, V_1 and V_2 have the values -5 meter sec^{-1} and -3.33 m sec^{-1} respectively for 0.5 km > z ≥ 0.

the surface. These conditions with V = constant comprise case 4; the same with a five fold increase in falling speed at the level of nondivergence is case 5. The V-discontinuity in case 5 resembles that accompanying the melting of snow. This model distribution is the condition of maximum precipitation rate at the updraft base for specified fall speed and maximum updraft. Above the level of nondivergence, no cloud exists, so none is lost by horizontal divergence; below the level of nondivergence, cloud condensed over a wide area is swept toward the updraft center, where it is collected by precipitation at the level of nondivergence and borne to the ground. Since precipitation cannot exceed condensation over a great region, excessive precipitation at the updraft center is accompanied by a balancing deficit away from the center. The one-dimensional cases imply the major features of two- and three-dimensional models required to satisfy conservation principles.

The computation of M-profiles in cases 4 and 5 involves some special considerations. From z = H to the level of nondivergence, M is given by an equation like (9). From z = 0 to the level of nondivergence, m is given by Eq. (8). At the level of nondivergence, precipitation M falling at velocity V + w collects all of the cloud m rising at speed w. Because conditions are steady, the value of M below the level of nondivergence is defined by equating the transport of M + m immediately below the level of nondivergence to the transport of M above that level; i.e.,

$$(mw)_{below} + [M(V + w)]_{below} = [M(V + w)]_{above} \qquad (10)$$

The updraft w has the same value immediately above and below the level of nondivergence.

Equation (10) has been applied to determination of the discontinuous M-profiles shown in Fig. 2, where the upper diagram pertains to constant G, cases 4a and 5a, and the lower to a linear distribution of G, cases 4b and 5b. Four profiles are

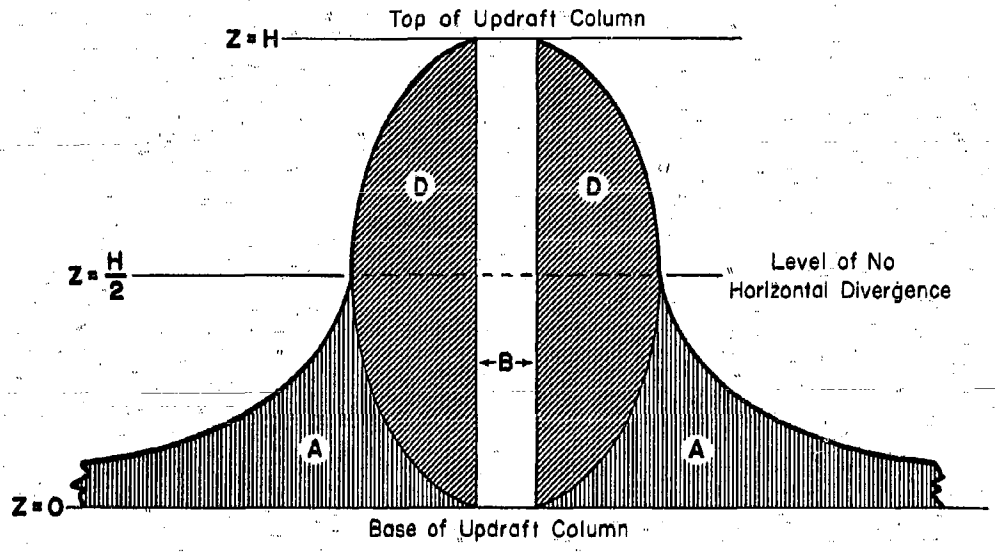

Fig. 3. Schematic illustration of Cases 3 and 4, discussed in the text and listed in Tables 3a, b and 4a, b. Horizontal divergence in the high atmosphere accompanies rising air motion and spreads precipitation packets horizontally as they descend in the shaded area marked D. The packets are contracted again by horizontal convergence in the lower atmosphere. Precipitation at the ground in the section marked B is due to condensation in a volume larger by the extent of horizontal shading than the unshaded cross section vertically overhead. When condensate augments precipitation at the level of nondivergence but not below that height, the region contributing to precipitation at B is further increased by the area of vertical shading marked A in the figure. Cloud in area A is swept inward and upward by horizontal convergence and ascends to the level of nondivergence, where it is collected by precipitation and ultimately deposited at the ground in Section B.

given in each diagram: two pertain to the cases in which V has constant values of -1 m/sec and -0.67 m/sec; the other two show the M-distribution that exists when each of these fall speeds increases by a factor of five at the level of non-divergence. Such a discontinuous change of V approximates the fall-speed changes that commonly occur at the melting level.

The profiles shown in Figs. 1 and 2 can be scaled to any distribution of atmospheric parameters that differ by constant factors from those used here. For new scale height H', new generating function G', new vertical air speed W_{max} and new fall speed $V' = W_{max} V/w_{max}$ the new solutions denoted by M' are given by $M' = M H'/GH$.

Principal features of the profiles in Figs. 1 and 2 are listed in Tables 1 through 5, which are numbered to correspond to case numbers of the figures. Note that Table 1 lists values of w and $\int wG\, dz$, which are the same for all the other tables. Note that the surface-precipitation rate exceeds the vertical integral of the condensation rate in practically all cases, and is more than five times the condensation term in the slow-fall-speed example of case 4b. Cases 3 and 4 considerably exaggerate the probable magnitude of the precipitation excess that characterizes centers of natural precipitation, since fall speeds in nature are usually much larger than updrafts. The mechanism responsible for the very high precipitation rates of case 4 is schematically illustrated in Fig. 3. Table 5 shows how the mechanism's effects are minimized when the fall speed increases during descent. This is discussed in some detail in [7].

1.3 Steady-state Vertical Distribution of Cloud in a Precipitation-free Compressible Atmosphere

The maximum possible cloud density at various atmospheric levels is a parameter of some importance to considerations of precipitation-cloud interactions. The steady distribution of cloud established in an air column after ascent has continued for a very long time without fallout of condensation products

also represents at each height the water content associated with ascent from the condensation level with retention of all cloud. The steady profile for a given condensation level thus represents the maximum attainable cloud content at each height for that condensation level.

In the steady state without cloud conversion of horizontal advection, Eq. (2) becomes

$$w \frac{\partial m}{\partial z} - mw \frac{\partial \ln \rho}{\partial z} - wG = 0 \tag{11}$$

or

$$\frac{\partial m}{\partial z} - m \frac{\partial \ln \rho}{\partial z} = G \tag{12}$$

Since w does not appear in Eq. (12) the solution, as expected, is independent of the shape of the updraft distribution. We assume $G = A + Bz$, and take $\frac{\partial \ln \rho}{\partial z} = K$, a constant. These are reasonable approximations to the real atmosphere. Then the solution of Eq. (12) is

$$m = e^{K(z - z_0)} \left[m_0 + \frac{1}{K} \left(A + Bz_0 + \frac{B}{K}\right) \right] - \frac{1}{K} \left(A + Bz + \frac{B}{K}\right). \tag{13}$$

In the tropical atmosphere $A \approx 3 \times 10^{-3}$ gm/m^4, $B \approx -3 \times 10^{-7}$ gm/m^5, and $K \approx -10^{-4}$ m^{-1}; substitution of these values in Eq. (13) yields:

$$m = e^{10^{-4}(z_0 - z)} \left[m_0 - 60 + 3 \times 10^{-3} z_0\right] + \left[60 - 3 \times 10^{-3} z\right]. \tag{14}$$

The units of m are gm meter^{-3} when z is given in meters.

The location of maxima of m are also of importance. Set $\frac{\partial m}{\partial z} = 0$ in Eq. (12) and integrate, and substitute for G and $\frac{\partial \ln \rho}{\partial z}$ as noted above. The height z where m is a maximum is the solution of Eq. (15).

$$e^{10^{-4}(z_0 - z)} = \frac{30}{60 - 3 \times 10^{-3} z_0} \tag{15}$$

Solutions represented by Eqs. (14) and (15) are plotted in Fig. 4. The height along each m- curve where $\frac{\partial m}{\partial z} = 0$, the compensation level, is for each condensation level z_c, the height where $m \frac{\partial \ln \rho}{\partial z} = -G$, i.e., where the tendency of the generating function to increase the density of condensate is exactly compensated by the decreasing density of ascending air. Above this level of compensation, cloud density decreases with ascent and increases with descent.

The generating function in this model is zero at and above 10 Km. Above 10 Km, therefore, the curves of Fig. 4 can be extended by use of the relationship

$$m(z) = m(10\ \text{Km})\ e^{10^{-4}\ (10^4 - z)} \qquad (16)$$

which is similar to that for the other atmospheric constituents not bound by the particular laws applicable to water substance.

This analysis may explain some of the vagaries of the association of high cloudiness with vertical air currents. When vertical currents carry an amount of cloud above the level of compensation for that cloud density, the cloud must be very persistent. Further ascent thins but does not dissipate it, while descent thickens it. Ascent increases the size of individual particles of condensate, but this is more than offset by their movement apart. The converse holds for descent of cloud between levels above the height of compensation. High level horizontal convergence and descending motion of a cloud layer isolated at levels above the height of compensation by effects of wind shear, could be associated with increasing cloud depth and density instead of the opposite so often assumed. Of course, Fig. 4 is inadequate for evaluating the probable importance of this effect in the real atmosphere, since the model generating function is only a rough approximation to the real one at the higher lev Furthermore, the cloud water content is in nature not controlled by the generating function and air density gradient alone, but by these with the depleting effects of precipitation. Observations show that

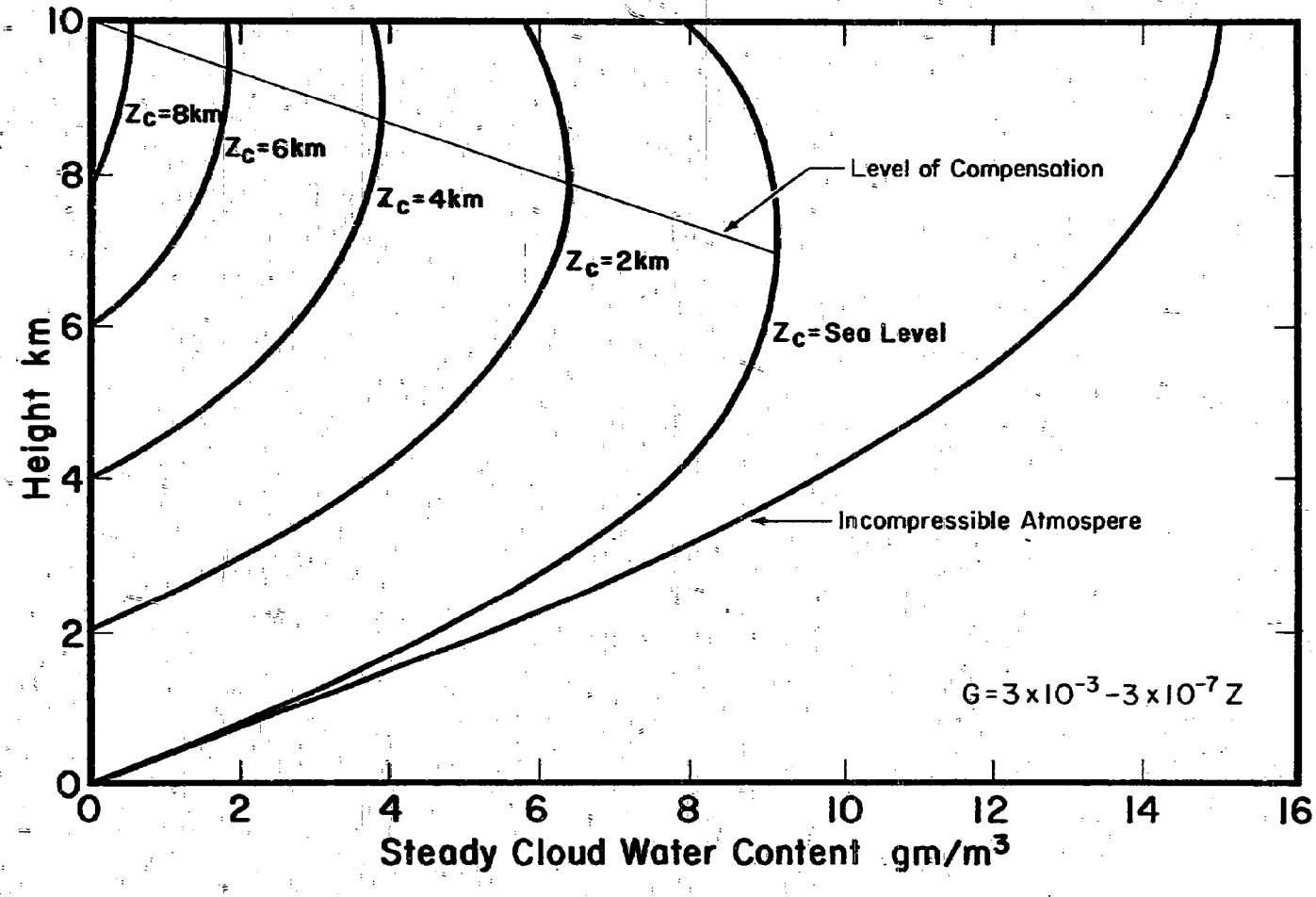

Fig. 4. Approximate cloud density in tropical air lifted without precipitation formation from various condensation levels, the intercepts of the curves with the vertical axis. The sloping straight line defines the height for each condensatio level and cloud amount above which cloud density decreases with rising motion. Extensions of the curves above 10 km follow an exponential decay law.

the values of Fig. 4 are much larger than usually occur. Therefore the effect of compressibility, which is proportional to m, must really be of less consequence than Fig. 4 implies. During the next quarter, a model generating function which more accurately represents the real tropical atmosphere, especially at high levels where G is very small but has great consequence for cirrus cloudiness, will be applied to an extension of this study.

1.4 Example Computer Solution of a One-dimensional Case with Cloud Conversion and Accretion

Quarterly Progress Report No. 1 of this contract discusses how the one-dimensional forms of Eqs. (1) and (2) for an incompressible atmosphere have been programmed for solution by digital computer.* During the past quarter, this program was used to compute the time-dependent vertical distributions of precipitation and cloud in an initially saturated atmosphere. The interaction terms in Eqs. (1) and (2) which are of importance here are

$$\frac{dM}{dt} \text{ or } -\frac{dm}{dt} = + K_1(m-a) \text{ gm m}^{-3}\text{sec}^{-1} \tag{17}$$

and

$$\frac{dM}{dt} \text{ or } -\frac{dm}{dt} = 6.96 \times 10^{-4} \, En_0^{0.125} \, mM^{.875} \text{ gm m}^{-3}\text{sec}^{-1}. \tag{18}$$

Eq. (17) refers to autoconversion of cloud to precipitation. Equation (18) refers to the collection of cloud by precipitation.

Also, in Eq. (2), the fall speed V is taken as the fall speed V_0 of the median volume diameter D_0:

$$V = V_0 = -38.6 \, n_0^{-0.125} \, M^{0.125} \text{ m sec}^{-1}. \tag{19}$$

*Although the discussion of Section 1.3 of this report demonstrates that the atmosphere's vertical variation of density may be an important factor for the cloud density at high altitudes, omission of the air density term is justified in the machine computations discussed here for two reasons: First, the effect of compressibility, proportional to cloud content, is small in these cases because the cloud content is depleted by precipitation to rather low values. Second, omission of the compressibility term provides more direct understanding of the role of the others. It is desirable to start with a simple model and to introduce refinements progressively.

The use of the cloud conversion term in Eq. (17) is not clearly supported or refuted by the literature, but seems necessary if a greater number of basic equations is to be avoided. Squires and Twomey [16], for example, suggest that important variations in cloud droplet concentrations and colloidal stability may occur as a result of variations of cloud nuclei content. In our initial selection of the value $a = 0.5$ gm m^{-3}, we have been guided by the literature that describes cloud water observations up to about 1 gm^{-3} where precipitation was not previously or subsequently observed [1, 15, 17]. The first choice of $K_1 = 10^{-3}$ sec^{-1} insures that substantial precipitation exists in the cloud 20 minutes after the cloud water content exceeds 0.5 gm/m^3. The magnitude of K_1 applicable in nature requires further clarification by reference to theoretical studies such as [12].

The derivation of Eq. (19) is discussed in Report No. 1. This equation defines the fall speed of the median-volume precipitation particle in the exponential number distribution comprising water content M and containing number n_0 per unit size range of zero-diameter particles. It is a little crude to assume as done here that the vertical flux is given by approximating the terminal fall speed of all the precipitation particles by the fall speed of the median particle. This has been shown by plotting the equation

$$M = M_0 n_0 \left(\frac{D}{D_0}\right)^3 e^{-3.75\, D/D_0} \qquad (20)$$

which relates the normalized mass distribution of particles in the Marshall-Palmer distribution to size $\frac{D}{D_0}$. Slightly more than 80% of the water content of the exponential distribution is represented by drop diameters D such that $.4D_0 < D < 1.6D_0$, i.e., a factor 4 in drop diameters. Since fall speed is proportional to the square root of drop diameter, there is a two fold variation of fall speed among the particle sizes which comprise 80% of the water content centered about D_0. In other words, fall speeds of 80% of the water content are in the

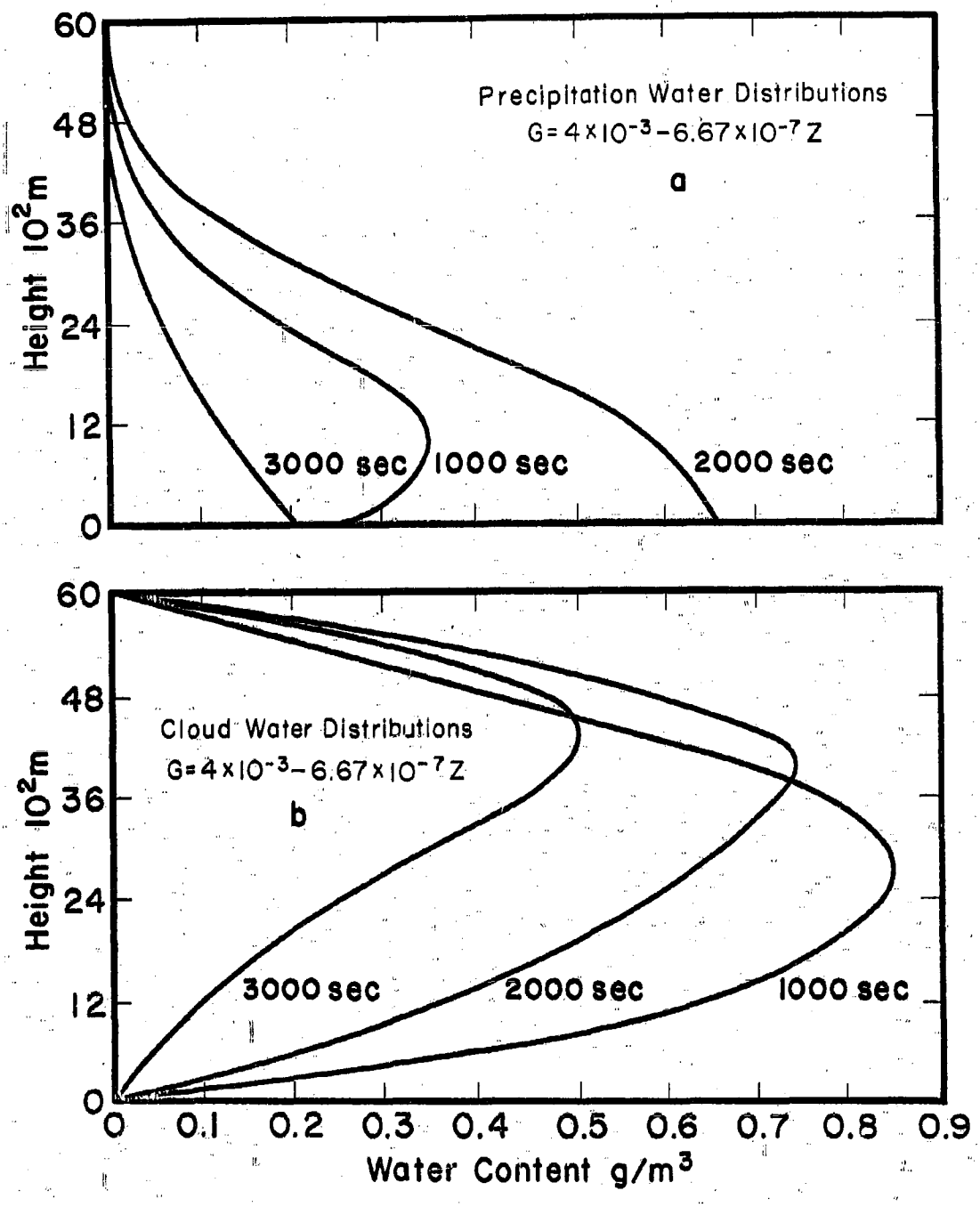

Fig. 5a. Vertical distributions of precipitation content at 1000, 2000, and 3000 seconds in the model defined by Table 6.

Fig. 5b. Vertical distributions of cloud content at 1000, 2000, and 3000 seconds in the model defined by Table 6.

TIME IN SECONDS

HEIGHT IN METERS	200	575	798	1260	1772	2000	3148
		Precip. Forms	Surface Rain Starts	Maximum Accretion Maximum Cloud Water	Maximum Surface Precip.	Updraft Stops	End of Calculation
6000							
5700							
5400							
5100							
4800							
4500							
4200							●3.93·10⁻¹
3900					●7.61·10⁻¹	●7.380·10⁻¹	
3600							
3300				●8.26·10⁻¹			
3000							
2700							
2400							■4.00·10⁻⁵
2100	●2.360·10⁻¹	■6.60·10⁻¹ ▲1.35·10⁻² ▼ 3.9	●8.10·10⁻¹				
1800			■5.58·10⁻⁴	■1.40·10⁻³	■1.22·10⁻³	■1.02·10⁻³	
1500			▲1.16·10⁻¹ ▼ 5.1				
1200							
900							
600				▲5.50·10⁻¹ ▼ 6.2			
300							
0			Rain Starts		▲6.63·10⁻¹ ▼ 6.4	▲6.58·10⁻¹ ▼ 6.3	▲1.01·10⁻¹ ▼ 5.0

m g/m³ ● Cloud Water Content

M g/m³ ▲ ▼ Precipitation Content and Fall Speed
V m/sec

g/m³ sec ■ Accretion of Cloud by Precipitation

Fig. 6. Distribution in height and time of significant space maxima in the cloud-precipitation model defined by Table 6. Note that the precipitation maximum increases as it descends; the cloud maximum decreases as it ascends. After the updraft ceases at 2000 seconds, the surface precipitation rate declines rapidly but the cloud aloft is relatively persistent.

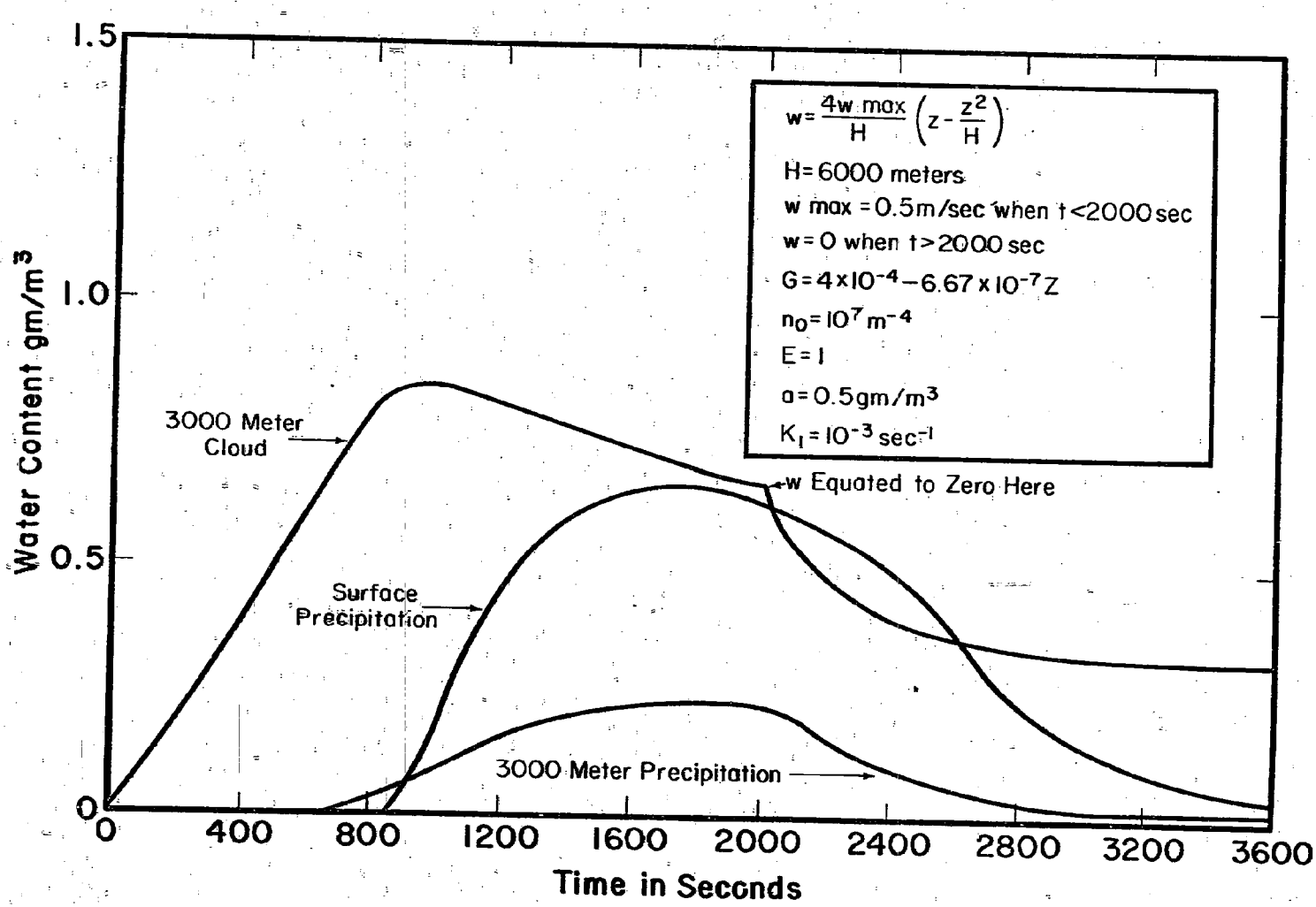

Fig. 7. Time dependence of the water content of cloud and precipitation at a height of 3000 meters at the center of an area where updrafts extend to 6000 meters. The variation of precipitation water content at the surface is also shown. This figure pertains to a linear distribution of the generating function, and should be compared with Fig. 1, Report No. 1 of this contract where results for a constant generating function are illustrated.

The figures show that the cloud water content first attains the value 0.5 gm/m^3 required for initial precipitation development, in the lower atmosphere slightly above the level where wG is a maximum. Once precipitation forms, it increases rapidly by collecting cloud. At early times, both cloud and precipitation have their maxima at the same height; cloud conversion and accretion proceed most rapidly at that height. The cloud collection process is responsible for the marked depletion of cloud in the lower atmosphere, for the steady downward shift of the precipitation maximum and the upward displacement of the cloud maximum. Note in Fig. 6 that the precipitation maximum progresses toward the surface at a rate of about 2 m/sec although the fall speed V_0 is typically 6 m/sec. The difference is important for the interpretation of radar observations. The radar reflectivity defined by this model has maxima and minima at the same places as M.

The solution of this problem shown in Fig. 7 should be compared to the case shown as Fig. 1 in Report No. 1 of this contract. The parameter values in the two cases are identical except for the distribution of G, a linear function of height in the present model and a constant in the former. The average value of G is the same in the two cases. Notice the similarity of the curves in Fig. 1 of Report No. 1 and Fig. 7 of this report. It is perhaps surprising that the solutions are not more affected by such a great change of the distribution of the generating function.

Note that the solutions are characterized by an initial pulse of precipitation and cloud content, then their decline to lesser values. The pulse is due to the choices of $a = 0.5\ gm/m^{-3}$ and $K_1 = .001\ sec^{-1}$, values which with the other parameters, lead to considerably higher cloud contents than can exist in equilibrium with generation and accretion processes. The cloud distribution after precipitation is initiated can hardly resemble the cloud distribution before. The onset of precipitation marks an alteration of the interplay of processes

affecting cloud distributions, which must persist until the circulation ceases and all precipitation has fallen from the cloud.

Note in Fig. 6 that precipitation spreads to levels above 4,800 meters where the cloud water content never reaches the value a = 0.5. Such spread of precipitation is an inherent feature of the finite difference computations. The precipitation content at any height z at time t + Δt is the mean of the values at z + Δz and z - Δz at time t, plus the changes due to advection and interaction processes computed for the time interval Δt. This computational method is necessary to guarantee that the answers are both computationally stable and better approximate the true solution to the differential equations as Δt and Δz become smaller.* The effects of averaging appear partly as a very slow depletion of cloud by precipitation even above levels where the spontaneous conversion of cloud to precipitation is active and even when V_0 is markedly greater than maximum updrafts. This manifestation probably has a natural analogue, since in any precipitation, however intense, there must exist some drops whose fall speeds are less than the updrafts, and which are carried upward with the updrafts.

1.5 Relationship of Precipitation Rate to the Updraft Intensity and to the Rate of Cloud Conversion

The parameter values in Table 7 have been used to test the effect of variations of updraft strength and rate of cloud conversion on the distributions of cloud and precipitation.

*Tests have shown how the solutions vary with choice of Δz and Δt. In the problem discussed here, a typical cloud or precipitation value at a given time is shifted 3% for a change of space discretization from 300 to 150 meters, 3% more for a change from 150 to 60 meters, but just 1% additional for a shift of Δz from 60 to 30 meters (200 steps). The use of 100 space steps seems a suitable compromise between accuracy and economy.

TABLE 7*

PARAMETER VALUES FOR STUDY OF EFFECTS OF UPDRAFT STRENGTH AND RATE OF CLOUD CONVERSION ON VERTICAL DISTRIBUTION OF PRECIPITATION AND CLOUD.

Case a)	$w_{max} = 0.5$ m/sec	$K_1 = 10^{-1}$ sec^{-1}
Case b)	$w_{max} = 0.5$ m/sec	$K_1 = 10^{-3}$ sec^{-1}
Case c)	$w_{max} = 0.5$ m/sec	$K_1 = 10^{-5}$ sec^{-1}
Cases d and e)	$w_{max} = 2.0$ m/sec	$K_1 = 10^{-3}$ sec^{-1}

*Parameters not identified here have been assigned the values given in Table 6 in Section 1.4 of this report.

The surface precipitation rates given by these models are depicted in Figs. 8 and 9. Figure 8 shows that the onset time of precipitation increases about 10 minutes for a decrease of K_1 by four orders of magnitude; the peak rate of rainfall increases only slightly for this enormous change of K_1. This type of finding may have some implications for cloud seeding efforts but should not be considered definitive at this stage of the work. The result seems astonishing when one considers Eq. (17) alone. With $K_1 = 10^{-5}$, about .01 of the cloud water in excess of the amount a spontaneously becomes precipitation after 1000 secs,† yet appreciable precipitation at the ground occurs in this model only 600 seconds later than in the case where spontaneous conversion of cloud water is 10,000 times faster. This result testifies to the effectiveness of accretion, Eq. (18), even when the amount of precipitation is very small.

This result should not be considered indicative of unimportance of the rate of cloud conversion in natural processes. Since a nonlinear relation between cloud conversion and collection governs the early rate of precipitation increase, substantial changes are probably associated with variations of K_1 when E and

†The amount of cloud water in this model which becomes precipitation in 1000 seconds by virtue of spontaneous cloud conversion alone is about .005 gm/m^3.

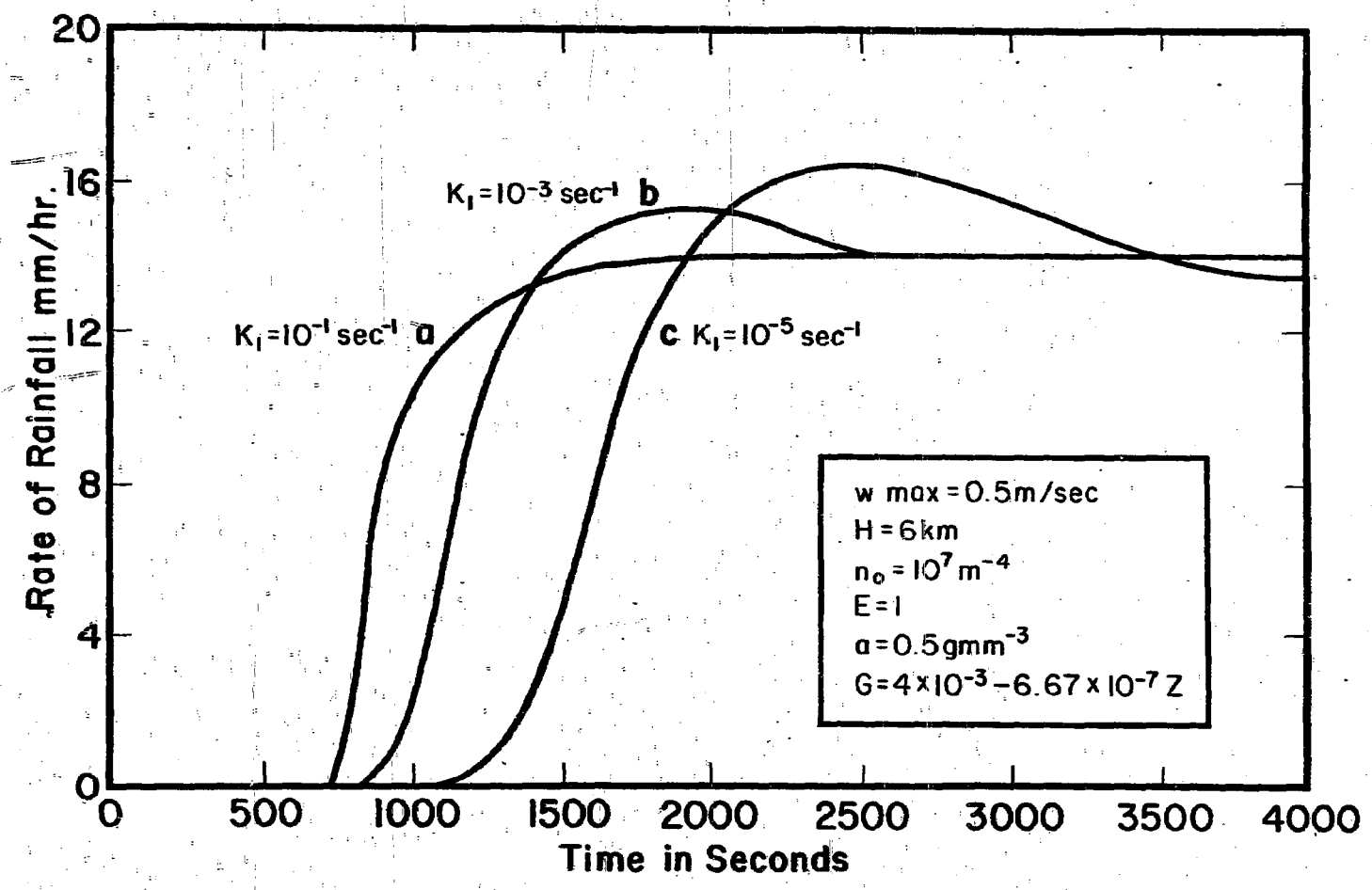

Fig. 8. Time dependence of surface precipitation rate as for three values of K, the rate at which cloud content in excess of the amount a changes spontaneously to precipitation. The sluggish variation of surface precipitation with very large changes of K indicates the great importance of the accretion process to comprehensive evaluation of the nex effects of cloud-precipitation interactions. (Case b computations terminated at 2600 secs.)

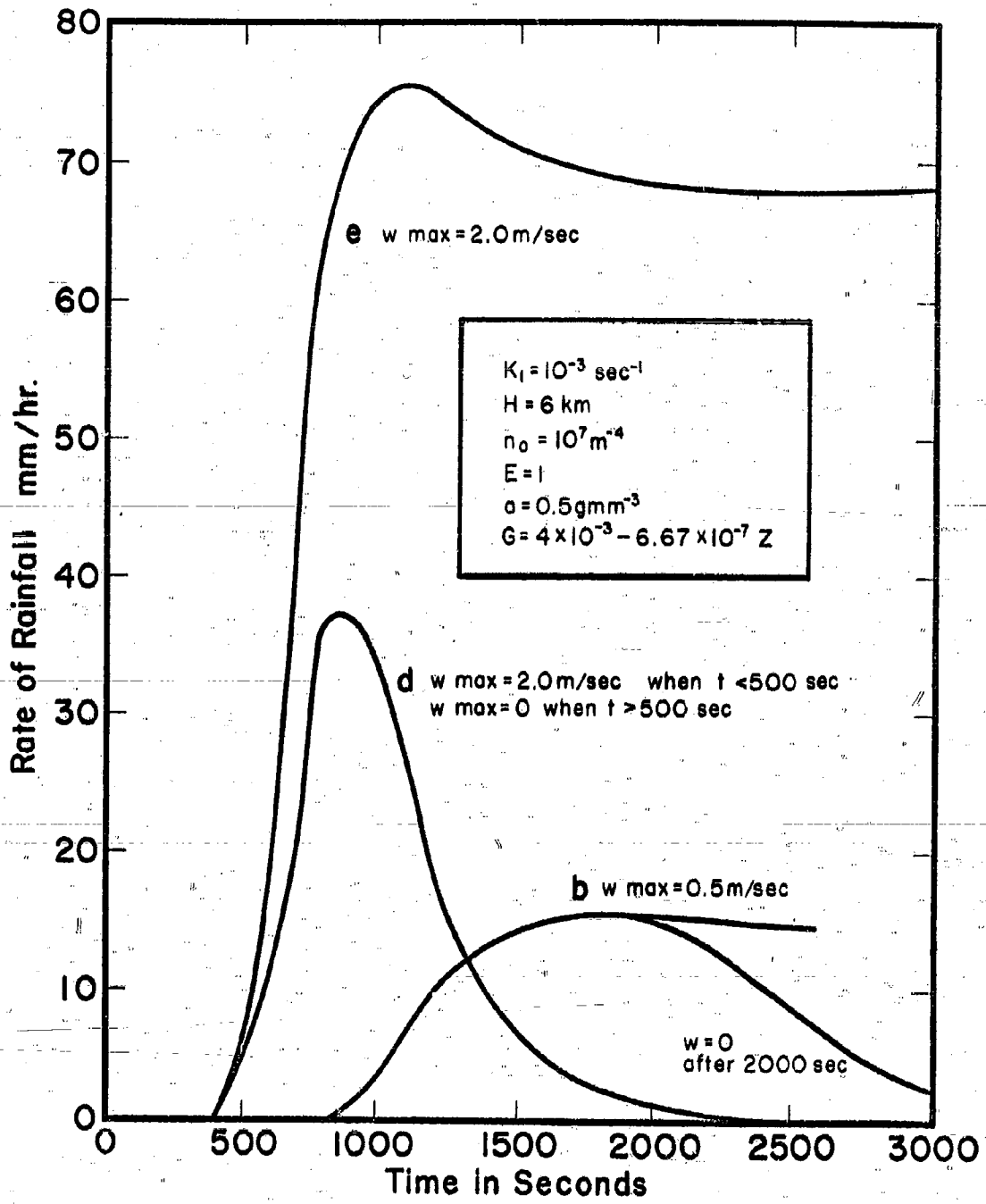

Fig. 9. Precipitation rate at the ground in three cases with $K_1 = 10^{-3}$ sec^{-1}. Case b, with continuing $w_{max} = 0.5$ m/sec, is the same as Case B in Fig. 10. Maximum updrafts are 2 m/sec in Cases d and e, continuing in Case e, but set to zero at 500 seconds in Case d.

n_0 lie within particular ranges. The Eqs. (17) and (18) can be combined to form a pair of differential equations with a straight-forward analytic solution which clearly illuminates the role of the equations' coefficients in precipitation initiation. These solutions are now being examined and will be discussed in the next report. Other theoretical work in precipitation physics [13, for example], is also being studied in order to derive estimates of K_1, n_0, and E which best model natural conditions. The variation of collection efficiency with size of precipitation particles affects both the constant coefficient and the exponent of M in Eq. (18).

At least one other property of the solutions shown in Fig. 8 is worthy of note. At 4000 seconds, the precipitation rates at the ground (and the distribution of cloud and precipitation aloft) are almost exactly the same in the three cases. However, the precipitation accumulated by 4000 seconds is 11.96 mm when $K_1 = 10^{-1}$ sec^{-1} and declines to just 10.08 mm when $K_1 = 10^{-5}$ sec^{-1}. The smaller value of K_1 is associated with longer initial duration of large amounts of cloud in the upper atmosphere where it is removed by horizontal divergence of the wind.

Figure 9 shows the precipitation rate at the ground in three cases of Table 7. Case b in Fig. 9 is the same as Case b in Fig. 8. The value of K_1 in Case d is the same as in b, but the maximum updrafts in Case d are 2m/sec and stop after 500 sec. Thus the amount of condensate produced in 2000 seconds in Case b equals that produced in 500 seconds in Case d. This amount on a level surface would have a depth of 8 mm. Now consider the precipitation totals received at the ground in two cases. By 2000 seconds, Case d produces 5.3 mm of precipitation at the surface; about .2 mm more falls after 2000 seconds for a total of 5.5 mm. Case b, on the other hand, produces only 3.5 mm of precipitation by 2000 seconds, but 2.5 mm falls after that time when the updrafts stop, for a total of 6.0 mm. Neither case produces as much as is condensed, since some condensate still remains as cloud aloft when computations are terminated,

and some condensate is lost by divergence at high levels during the time period before precipitation starts.

The greater efficiency of Case b than Case d can be understood in terms of the discussion given in connection with Eq. (7), Section 1.1. First, the low level convergence which acts to increase precipitation at updraft cores at the expense of amounts away from the core, is effective only if the precipitation descends through updrafts. In Case d, the updrafts stop before appreciable precipitation reaches the ground. Second, in the strong updraft case, cloud is lifted higher before it changes to precipitation; therefore a greater amount of cloud is removed from the updraft core by divergence in Case d than in Case b. To the extent that cloud is carried to greater heights by stronger updrafts and more spread out there by accompanying strong horizontal divergence, instead of descending to the ground as precipitation in the saturated updrafts, the stronger updraft cases are less efficient producers of precipitation than are the weak updraft models. Accurate evaluation of these effects will be possible when two- and three-dimensional models are programmed for the computer.

In Case e, 2 m/sec updrafts continue to 3000 secs. Note that the steady precipitation rate in this case is somewhat more than four times greater than the precipitation rate in Case b. That the steady precipitation rate is not exactly proportional to the updraft intensity is related to variations with updraft strength of the shape of the vertical distributions of cloud and precipitation and to changes of the proportional contribution of the divergence term in Eq. (7).

It is particularly worthy of note in these solutions, as in others not reproduced here, that the transient effects manifested in the surface precipitation rates by the simulated cloud physics processes are rather small. The surface precipitation rate is mightily dependent on the updrafts, however. Part of our task during the next interval will be to learn if there are parameter combinations which produce larger oscillations or other transient effects with steady updrafts than the weak variations computed thus far.

1.6 Comment on Mathematical Background

The mathematical background of the equations employed in this study has been investigated starting with the one-dimensional cloud-free model where the fall speed of condensate is constant [7, 8]. The existence and uniqueness of the solutions presented and discussed in the references from a physical standpoint is rigorously demonstrated below.

The one-dimensional cloud-free equation is

$$\frac{\partial M}{\partial t} + (V + w)\frac{\partial M}{\partial z} = wG \tag{21}$$

in which V is constant;

$$w = az(H - z) \tag{22}$$

and G is a differentiable function of z alone. Equation (21) is to be solved in the strip

$$S: 0 \leq z \leq H; \qquad 0 \leq t < +\infty$$

subject to the conditions

$$M(z, 0) = 0$$
$$M(H, t) = 0 \tag{23}$$

and

$$V + w < 0 \tag{24}$$

The physical meaning of Eq. (24) is that updrafts are everywhere less than the precipitation falling speed. The problem as posed has a continuous unique solution, proved as follows. The characteristic equations of (1) are

$$\frac{dt}{ds} = 1; \quad \frac{dz}{ds} = V + w; \quad \frac{dM}{ds} = wG \tag{25}$$

Through each point of the interval

$$t = 0, \quad 0 \leq z \leq H; \quad M = 0, \tag{26}$$

will pass a unique continuous solution of Eq. (25) subject to the initial conditions

$$t = M = 0$$
$$z = z_0 \qquad (0 \leq z_0 \leq H) \tag{27}$$

and through each point of the half-line

$$z = H, \qquad 0 \leq t < +\infty, \qquad M = 0 \tag{28}$$

will pass a unique solution subject to the initial conditions

$$z = H, \qquad M = 0$$
$$t = t_0 \qquad (0 \leq t_0 < +\infty). \tag{29}$$

The uniqueness and existence of the solutions follow from standard existence theorms [5] since the right sides of Eq. (25) are continuous and Lipschitzian.

In the t - z plane, the characteristic base curves for Eq. (21) are determined from

$$\frac{dz}{dt} = V + w \tag{30}$$

together with proper initial conditions. These base curves cover the strip S in the sense that through each point in the strip passes one and only one base curve. Each of these curves intersects one or the other, but not both, of the intervals (26) and (28) in one and only one point. These facts follow from Eq. (24) and the Lipschitzian character of $V_t + w$. With each point on a base curve in the strip S there is associated a unique value of M determined from (25) with the proper initial point. The M associated in this manner with each point in the strip S determines a unique continuous solution of (21) which satisfies (23) as follows from the standard theory of linear partial differential equations in two independent variables [3].

The method of solution is summarized as follows. To determine the value of M at the point (z_1, t_1) in the strip S, solve (30) to determine the characteristic base curve which goes through (z_1, t_1). Call this curve C_1. Find the point of intersection of C_1 with either (26) or (28) as the case may be. Call this point (z_0, t_0). Determine M from (25) by solving for M as a function of z from

$$\frac{dM}{dz} = \frac{wG}{V + w} \tag{31}$$

with $M(z_0) = 0$, and setting $z = z_1$.

One should notice that the characteristic base curve which goes through the point $t = 0$, $z = H$ divides the strip S into two regions: one to the right (t increasing) and one to the left (t decreasing) of the base curve. For points in the strip which lie to the right of this curve, the value of z_0 of the above paragraph is always H and the solution of (31) is independent of t. That is, the solution of (21) under conditions (23) and (24) in the strip S attains a steady state for which $\partial M/\partial t = 0$ for z fixed.

An interesting variation of the problem considered above is defined by conditions

$$\begin{array}{lll} V + w < 0 & 0 \leq z < h_1 & h_2 < z \leq H \\ V + w = 0 & z = h_1, h_2 & \\ V + w > 0 & h_1 < z < h_2 & \end{array} \qquad (32)$$

The conditions (32) mean that the maximum updraft exceeds the precipitation fall speed. Application of the previous reasoning to each of the three strips in the $t - z$ plane determined by (32) for $t \geq 0$ leads to the conclusion that there exists a unique continuous solution of (21) for $0 \leq z \leq H$, $t \geq 0$, which satisfies (23) under conditions (32). Consideration of the characteristic base curves of (21) for this problem shows that for any fixed $z > h_2$ there is a time beyond which the solution is steady. For any $z > h_2$, there is no steady-state solution. This case is discussed from a physical point of view in [8].

The question of existence and uniqueness for the quasi-linear hyperbolic system describing clouds and rain cannot be answered at present. It is a reasonable conjecture that a unique continuously differentiable solution does not exist for conditions of M, m = 0 initially. R. Courant [2] has recently established the existence of a continuously differentiable solution for the hyperbolic system, $u_t + A(x, t, u)\, u_x + B(x, t, u) = 0$, with initial data $u(x, 0) = \Psi(x)$ on some interval of the x- axis. His method of proof requires that $A(x, t, u)$ and $B(x, t, u)$ be continuously differentiable in the domain of

x, t, u under consideration. Our problem fails to satisfy this condition.

Since Courant's proof follows from the weakest hypotheses deemed reasonable for success in solving the problem, it is felt that a unique solution for the equations of clouds and rain must perforce be a generalized solution which allows discontinuities in the derivatives of the solution vector. We believe that a solution of this type might be established along the lines followed by Kuznecov and Rozdestvenskii [10]. However, due to the rather abstract and purely mathematical nature of this problem it is felt that no further effort should be devoted to it on this contract.

The incomplete theory of the techniques used in this investigation is not satisfying to a mathematician. However, this fact is not cause for rejection of the results of the computations. The physical reasoning underlying the mathematical formulation of this problem and the numerical results of these and similar calculations of others (e.g., P. D. Lax [3]) imply strong credibility for the results. The semi-empirical approach used here is typical in the development of new methods. As R. D. Richtmyer [4] has said, "... if we were to wait for convergence proofs and error estimates for the new methods, most of the computers now in use in technology and industry would come grinding to a halt."

1.7 The Difference Between the Horizontal Speed of Raindrops and the Horizontal Wind Speed.

The precipitation-cloud models discussed in this report are based in part on the assumption that the horizontal speed of condensate is the same as the horizontal speed of the air. The validity of this assumption must decrease with increasing size of precipitation particles; a fair test of this assumption is therefore given by examination of an equation of motion for a large raindrop.

The horizontal resisting force on a spherical raindrop is given by

$$f_r = 6\pi\mu r(u - v)\frac{C_D R_e}{24} \qquad (83)$$

where μ is the viscosity of air, r is the radius of the drop, u is the horizontal velocity of the air, v is the horizontal velocity of the drop, C_D is the drag coefficient, and R_e is the Reynold's number [6, p. 121]. Consider a drop falling at terminal speed through a layer of vertical shear of the horizontal wind. The drop is accelerating horizontally due to the force associated with a difference between its horizontal velocity and the horizontal air motion. This force given by Eq. (33) is equal to the mass of the drop times its horizontal acceleration, i.e.,

$$6\pi\mu r\,(u - v)\,\frac{C_D R_e}{24} = \frac{4\pi}{3}\,r^3\rho\,\frac{dv}{dt}, \tag{34}$$

where ρ is the density of water. Consider a drop of radius 0.24 cm. The quantity $C_D R_e/24 \approx 77$ and $\mu \approx 1.8 \times 10^{-4}$ gm cm^{-1} sec^{-1}. Substitute these values in (34) to obtain

$$\frac{dv}{dt} = 1.09\,(u - v). \tag{35}$$

Nothing of importance to this development is lost by considering the case where the shear is uniform and the difference between the horizontal wind speed and drop speed is constant. The drop's falling speed, about 907 cm sec^{-1} and the shear $\partial u/\partial z = B$ determines du/dt, the time rate of change of u (and v) at the drop.

$$\frac{du}{dt} = \frac{dv}{dt} = \frac{dz}{dt}\,\frac{\partial u}{\partial z} = 907B. \tag{36}$$

Substitute for dv/dt in (35) from (36) to get

$$u - v = \frac{907B}{1.09}. \tag{37}$$

When B is 0.02 sec^{-1} (20 m/sec km, a very large value), u - v is only 16.64 cm/sec, less than 1% of representative horizontal wind speeds.

So long as u - v is small compared with the terminal fall speeds, the method employed here yields an accurate measure of u - v. The generalization to variable shear and variable u - v is obvious but of little practical interest

to the work of the contract since u - v is so small. The work of Das [4, Table 1 and app.], brought to our attention after that above had been completed, leads by a different path to the same conclusion.

1.8 REFERENCES

1. Ackerman, B., "The Variability of Liquid Water Content of Tropical Cumuli," J. Meteorol. 16:2, 191–198 (1959).

2. Courant, R., "Cauchy's Problem for Hyperbolic Quasi-linear Systems of First Order Partial Differential Equations in Two Independent Variables," Communs. Pure and Appl. Math. 14:3, 257–265 (1961).

3. — and Hilbert, "Partial Differential Equations," Methods of Mathematical Physics, vol. II. New York: Interscience, 1962.

4. Das, P., "Influence of Wind Shear on the Growth of Hail," J. Atmos. Sci. 19:5, 407–414 (1962).

5. Ince, E. L., Ordinary Differential Equations. London: Longmans Green & Co. Reprinted by Dover Publications, New York.

6. Johnson, J. C., Physical Meteorology. New York: John Wiley & Sons, 1954.

7. Kessler, E. III, "Kinematical Relations Between Wind and Precipitation Distributions," J. Meteorol. 16:6, 630–637 (1959).

8. —, "Kinematical Relations Between Wind and Precipitation Distributions, II," J. Meteorol. 18:4, 510–525 (1961).

9. —, "Elementary Theory of Associations Between Atmospheric Motions and Distributions of Water Content," Mo. Weath. Rev. (to be published in Jan. 1963).

10. Kuznecov, N. N., and B. Z. Rozdestvenskii, "Existence and Uniqueness of the Generalized Solution of the Cauchy Problem for a Non-homogeneous Law of Conservation," Doklady Akad. Nauk.S.S.S.R. 126 (1959) (in Russian).

11. Lax, P. D., "Weak Solutions of Nonlinear Hyperbolic Equations and their Numerical Computation," Communs. Pure and Appl. Math. 7, 159–193 (1954).

12. Marshall, J. S., and W. McK. Palmer, "The Distribution of Raindrops with Size," J. Meteorol. 5:4, 165-166 (1948).

13. Neiburger, M., and C. W. Chien, "Computations of the Growth of Cloud Drops by Condensation Using an Electronic Digital Computer," Geophys. Monogr. pp. 191-210, Am. Geophys. Un., 1960.

14. Richtmyer, R. D., Difference Methods for Initial Value Problems, p. vi. New York: Interscience Publishers, Inc. 1957.

15. Singleton, F., and D. J. Smith, "Some Observations of Drop Size Distributions in Low Layer Clouds," Quart. J. Roy. Meteorol. Soc. 86:370, 454-467 (1960).

16. Squires, P., and S. Twomey, "The Relation Between Cloud Drop Spectra and the Spectrum of Cloud Nuclei," Geophys. Monogr. no. 5, pp. 211-219, Am. Geophys. Un. Washington 5, D.C., 1960.

17. Weickmann, H. K., and H. J. aufm Kampe, "Physical Properties of Cumulus Clouds," J. Meteorol. 10:3, 204-211 (1953).

2.0 CONCLUSION

The basic formulation, Eqs. (1) and (2), is a valuable tool for investigation of the macroscopic effects of cloud physics processes and of fundamental properties of associations between wind and condensate distributions. Solutions indicate much about the extent of control exercised by the cloud physics processes on the shapes of cloud and precipitation distributions and on precipitation intensity.

3.0 PROGRAM FOR NEXT INTERVAL

The investigative program during the next interval should include study in the following areas, not all of which will be concluded.

1. Accurate determination of the profile of saturation water vapor density in the tropical atmosphere, especially at high levels, and examination of the implications of this distribution for the persistence of high cloud (Section 1.3).

2. Study of literature pertinent to selection of cloud conversion coefficients and collection efficiencies representative of the real atmosphere (Sections 1.4 and 1.5).

3. Examination of the simultaneous analytic solutions of equations modeling the time dependence of m and M in the presence of cloud conversion and accretion processes, and analysis of the role of cloud conversion and accretion coefficients in shaping precipitation development (Section 1.5).

4. Evaluation of the roles of the shape of the distribution of precipitation particles and of the critical cloud water content for the intensity and time dependence of surface precipitation and vertical profiles of precipitation and cloud. This work will proceed by examination of the computer solutions for selected combinations of n_0 and a (Section 1.5).

5. Preparation of a computer program for two dimensional and radially symmetric models with provisions for computation of cloud, precipitation, and vapor budgets within the atmospheric volume.

4.0 IDENTIFICATION OF PERSONNEL

4.1 Extent of Participation

Name	Title	Total hours worked during the quarter (approximate)
E. Kessler	Principal Investigator	160
P. J. Feteris	Research Scientist (Meteorologist)	330
E. A. Newburg	Research Scientist (Mathematician)	135
C. P. Robson	Research Associate (Programmer)	30
G. Wickham	Research Associate (Programmer)	130
P. Duchow	Senior Research Aide	70

Secretarial, administrative, and drafting assistance was also provided. Mr. Feteris joined the project on August 6, 1962.

4.2 Biography of Pieter J. Feteris

Mr. Feteris is a research Scientist in the Atmospheric Physics Division of The Travelers Research Center, Inc. He is taking part in the analysis and development of cloud and precipitation models and is also engaged in a statistical study to relate the statistical properties of radar patterns to pattern predictability.

From 1957 to 1962 he was Junior Scientific Officer at the Royal Netherlands Meteorological Institute, where he made weather analyses and issued shipping forecasts.

Mr. Feteris attended Leiden University and the Imperial College at London and he received his MS in Meteorology from The University of London in 1956.

He is also a foreign member of the Royal Meteorological Society.

AD__________ Accession No.__________

The Travelers Research Center, Inc.
Hartford 3, Connecticut

RELATIONSHIPS BETWEEN TROPICAL PRECIPITATION AND KINEMATIC CLOUD MODELS (Rpt. 2)

Edwin Kessler, III, Pieter J. Feteris, and Edward A. Newburg

2nd Quart. Progress Rpt., 1 Aug. 1962–31 Oct. 1962. 37pp. incl. 9 figs., 5 tables, 17 refs. Contract DA 36-039 SC 89099. DA Proj. 3A 99-27-005. UNCLASSIFIED report.

A system of conservation equations embodying conversion of cloud to precipitation and cloud collection by precipitation are examined. The steady precipitation rate at the base of a model updraft column is shown to be a maximum when cloud conversion and collection are complete above the level of nondivergence and zero below that level. The decrease of saturation vapor density with height, characteristic of the atmosphere, implies that for any cloud-water content, there is a level (compensation level) above which the cloud density decreases with ascending motion, and conversely. For a particular choice of the magnitude of cloud collection, the precipitation rate at the ground and its time of onset is rather insensitive to the rate of cloud conversion. The efficiency of precipitation production at the earth's

UNCLASSIFIED

1. Atmosphere models
2. Convection
3. Precipitation
4. Cloud
5. Contract DA 36-039 SC 89099

AD__________ Accession No.__________

The Travelers Research Center, Inc.
Hartford 3, Connecticut

RELATIONSHIPS BETWEEN TROPICAL PRECIPITATION AND KINEMATIC CLOUD MODELS (Rpt. 2)

Edwin Kessler, III, Pieter J. Feteris, and Edward A. Newburg

2nd Quart. Progress Rpt., 1 Aug. 1962–31 Oct. 1962. 37pp. incl. 9 figs., 5 tables, 17 refs. Contract DA 36-039 SC 89099. DA Proj. 3A 99-27-005. UNCLASSIFIED report.

A system of conservation equations embodying conversion of cloud to precipitation and cloud collection by precipitation are examined. The steady precipitation rate at the base of a model updraft column is shown to be a maximum when cloud conversion and collection are complete above the level of nondivergence and zero below that level. The decrease of saturation vapor density with height, characteristic of the atmosphere, implies that for any cloud-water content, there is a level (compensation level) above which the cloud density decreases with ascending motion, and conversely. For a particular choice of the magnitude of cloud collection, the precipitation rate at the ground and its time of onset is rather insensitive to the rate of cloud conversion. The efficiency of precipitation production at the earth's

UNCLASSIFIED

1. Atmosphere models
2. Convection
3. Precipitation
4. Cloud
5. Contract DA 36-039 SC 89099

AD__________ Accession No.__________

The Travelers Research Center, Inc.
Hartford 3, Connecticut

RELATIONSHIPS BETWEEN TROPICAL PRECIPITATION AND KINEMATIC CLOUD MODELS (Rpt. 2)

Edwin Kessler, III, Pieter J. Feteris, and Edward A. Newburg

2nd Quart. Progress Rpt., 1 Aug. 1962–31 Oct. 1962. 37pp. incl. 9 figs., 5 tables, 17 refs. Contract DA 36-039 SC 89099. DA Proj. 3A 99-27-005. UNCLASSIFIED report.

A system of conservation equations embodying conversion of cloud to precipitation and cloud collection by precipitation are examined. The steady precipitation rate at the base of a model updraft column is shown to be a maximum when cloud conversion and collection are complete above the level of nondivergence and zero below that level. The decrease of saturation vapor density with height, characteristic of the atmosphere, implies that for any cloud-water content, there is a level (compensation level) above which the cloud density decreases with ascending motion, and conversely. For a particular choice of the magnitude of cloud collection, the precipitation rate at the ground and its time of onset is rather insensitive to the rate of cloud conversion. The efficiency of precipitation production at the earth's

UNCLASSIFIED

1. Atmosphere models
2. Convection
3. Precipitation
4. Cloud
5. Contract DA 36-039 SC 89099

AD__________ Accession No.__________

The Travelers Research Center, Inc.
Hartford 3, Connecticut

RELATIONSHIPS BETWEEN TROPICAL PRECIPITATION AND KINEMATIC CLOUD MODELS (Rpt. 2)

Edwin Kessler, III, Pieter J. Feteris, and Edward A. Newburg

2nd Quart. Progress Rpt., 1 Aug. 1962–31 Oct. 1962. 37pp. incl. 9 figs., 5 tables, 17 refs. Contract DA 36-039 SC 89099. DA Proj. 3A 99-27-005. UNCLASSIFIED report.

A system of conservation equations embodying conversion of cloud to precipitation and cloud collection by precipitation are examined. The steady precipitation rate at the base of a model updraft column is shown to be a maximum when cloud conversion and collection are complete above the level of nondivergence and zero below that level. The decrease of saturation vapor density with height, characteristic of the atmosphere, implies that for any cloud-water content, there is a level (compensation level) above which the cloud density decreases with ascending motion, and conversely. For a particular choice of the magnitude of cloud collection, the precipitation rate at the ground and its time of onset is rather insensitive to the rate of cloud conversion. The efficiency of precipitation production at the earth's

UNCLASSIFIED

1. Atmosphere models
2. Convection
3. Precipitation
4. Cloud
5. Contract DA 36-039 SC 89099

surface by transient disturbances in a saturated model atmosphere decreases with increasing speed of the updraft. Paths for further study of the role of cloud conversion and cloud collection processes for the initiation of precipitation are indicated. The difference oetween the horizontal speed of raindrops and the horizontal wind speed is almost always less than 1% of representative horizontal winds.

surface by transient disturbances in a saturated model atmosphere decreases with increasing speed of the updraft. Paths for further study of the role of cloud conversion and cloud collection processes for the initiation of precipitation are indicated. The difference between the horizontal speed of raindrops and the horizontal wind speed is almost always less than 1% of representative horizontal winds.

surface by transient disturbances in a saturated model atmosphere decreases with increasing speed of the updraft. Paths for further study of the role of cloud conversion and cloud collection processes for the initiation of precipitation are indicated. The difference between the horizontal speed of raindrops and the horizontal wind speed is almost always less than 1% of representative horizontal winds.

surface by transient disturbances in a saturated model atmosphere decreases with increasing speed of the updraft. Paths for further study of the role of cloud conversion and cloud collection processes for the initiation of precipitation are indicated. The difference between the horizontal speed of raindrops and the horizontal wind speed is almost always less than 1% of representative horizontal winds.

AD________________ Accession No.________________

The Travelers Research Center, Inc.
Hartford 3, Connecticut

RELATIONSHIPS BETWEEN TROPICAL PRECIPITATION AND KINEMATIC CLOUD MODELS (Rpt. 2)

Edwin Kessler, III, Pieter J. Feteris, and Edward A. Newburg

2nd Quart. Progress Rpt., 1 Aug. 1962–31 Oct. 1962. 37pp. incl. 9 figs., 5 tables, 17 refs. Contract DA 36-039 SC 89099. DA Proj. 3A 99-27-005. UNCLASSIFIED report.

A system of conservation equations embodying conversion of cloud to precipitation and cloud collection by precipitation are examined. The steady precipitation rate at the base of a model updraft column is shown to be a maximum when cloud conversion and collection are complete above the level of nondivergence and zero below that level. The decrease of saturation vapor density with height, characteristic of the atmosphere, implies that for any cloud-water content, there is a level (compensation level) above which the cloud density decreases with ascending motion, and conversely. For a particular choice of the magnitude of cloud collection, the precipitation rate at the ground and its time of onset is rather insensitive to the rate of cloud conversion. The efficiency of precipitation production at the earth's

UNCLASSIFIED

1. Atmosphere models
2. Convection
3. Precipitation
4. Cloud
5. Contract DA 36-039 SC 89099

AD________________ Accession No.________________

The Travelers Research Center, Inc.
Hartford 3, Connecticut

RELATIONSHIPS BETWEEN TROPICAL PRECIPITATION AND KINEMATIC CLOUD MODELS (Rpt. 2)

Edwin Kessler, III, Pieter J. Feteris, and Edward A. Newburg

2nd Quart. Progress Rpt., 1 Aug. 1962–31 Oct. 1962. 37pp. incl. 9 figs., 5 tables, 17 refs. Contract DA 36-039 SC 89099. DA Proj. 3A 99-27-005. UNCLASSIFIED report.

A system of conservation equations embodying conversion of cloud to precipitation and cloud collection by precipitation are examined. The steady precipitation rate at the base of a model updraft column is shown to be a maximum when cloud conversion and collection are complete above the level of nondivergence and zero below that level. The decrease of saturation vapor density with height, characteristic of the atmosphere, implies that for any cloud-water content, there is a level (compensation level) above which the cloud density decreases with ascending motion, and conversely. For a particular choice of the magnitude of cloud collection, the precipitation rate at the ground and its time of onset is rather insensitive to the rate of cloud conversion. The efficiency of precipitation production at the earth's

UNCLASSIFIED

1. Atmosphere models
2. Convection
3. Precipitation
4. Cloud
5. Contract DA 36-039 SC 89099

AD________________ Accession No.________________

The Travelers Research Center, Inc.
Hartford 3, Connecticut

RELATIONSHIPS BETWEEN TROPICAL PRECIPITATION AND KINEMATIC CLOUD MODELS (Rpt. 2)

Edwin Kessler, III, Pieter J. Feteris, and Edward A. Newburg

2nd Quart. Progress Rpt., 1 Aug. 1962-31 Oct. 1962. 37pp. incl. 9 figs., 5 tables, 17 refs. Contract DA 36-039 SC 89099. DA Proj. 3A 99-27-005. UNCLASSIFIED report.

A system of conservation equations embodying conversion of cloud to precipitation and cloud collection by precipitation are examined. The steady precipitation rate at the base of a model updraft column is shown to be a maximum when cloud conversion and collection are complete above the level of nondivergence and zero below that level. The decrease of saturation vapor density with height, characteristic of the atmosphere, implies that for any cloud-water content, there is a level (compensation level) above which the cloud density decreases with ascending motion, and conversely. For a particular choice of the magnitude of cloud collection, the precipitation rate at the ground and its time of onset is rather insensitive to the rate of cloud conversion. The efficiency of precipitation production at the earth's

UNCLASSIFIED

1. Atmosphere models
2. Convection
3. Precipitation
4. Cloud
5. Contract DA 36-039 SC 89099

AD________________ Accession No.________________

The Travelers Research Center, Inc.
Hartford 3, Connecticut

RELATIONSHIPS BETWEEN TROPICAL PRECIPITATION AND KINEMATIC CLOUD MODELS (Rpt. 2)

Edwin Kessler, III, Pieter J. Feteris, and Edward A. Newburg

2nd Quart. Progress Rpt., 1 Aug. 1962–31 Oct. 1962. 37pp. incl. 9 figs., 5 tables, 17 refs. Contract DA 36-039 SC 89099. DA Proj. 3A 99-27-005. UNCLASSIFIED report.

A system of conservation equations embodying conversion of cloud to precipitation and cloud collection by precipitation are examined. The steady precipitation rate at the base of a model updraft column is shown to be a maximum when cloud conversion and collection are complete above the level of nondivergence and zero below that level. The decrease of saturation vapor density with height, characteristic of the atmosphere, implies that for any cloud-water content, there is a level (compensation level) above which the cloud density decreases with ascending motion, and conversely. For a particular choice of the magnitude of cloud collection, the precipitation rate at the ground and its time of onset is rather insensitive to the rate of cloud conversion. The efficiency of precipitation production at the earth's

UNCLASSIFIED

1. Atmosphere models
2. Convection
3. Precipitation
4. Cloud
5. Contract DA 36-039 SC 89099

surface by transient disturbances in a saturated model atmosphere decreases with increasing speed of the updraft. Paths for further study of the role of cloud conversion and cloud collection processes for the initiation of precipitation are indicated. The difference between the horizontal speed of raindrops and the horizontal wind speed is almost always less than 1% of representative horizontal winds.

surface by transient disturbances in a saturated model atmosphere decreases with increasing speed of the updraft. Paths for further study of the role of cloud conversion and cloud collection processes for the initiation of precipitation are indicated. The difference between the horizontal speed of raindrops and the horizontal wind speed is almost always less than 1% of representative horizontal winds.

surface by transient disturbances in a saturated model atmosphere decreases with increasing speed of the updraft. Paths for further study of the role of cloud conversion and cloud collection processes for the initiation of precipitation are indicated. The difference between the horizontal speed of raindrops and the horizontal wind speed is almost always less than 1% of representative horizontal winds.

surface by transient disturbances in a saturated model atmosphere decreases with increasing speed of the updraft. Paths for further study of the role of cloud conversion and cloud collection processes for the initiation of precipitation are indicated. The difference between the horizontal speed of raindrops and the horizontal wind speed is almost always less than 1% of representative horizontal winds.

DISTRIBUTION LIST

Address	No. of Copies
ARDC Liaison Office, U.S. Army Electronics Research and Development Laboratory, ATTN: SELRA/SL-LNA, Fort Monmouth, New Jersey	1
U.S. Navy Electronics Liaison Office, U.S. Army Electronics Research & Development Laboratory, ATTN: SELRA/SL-LNS, Fort Monmouth, New Jersey	1
USCONARC Liaison Office, U.S. Army Electronics Research & Development Laboratory, ATTN: SELRA/SL-LNP, Fort Monmouth, New Jersey	1
Commanding Officer, U.S. Army Electronics Research & Development Laboratory, ATTN: SELRA/SL-DR, Fort Monmouth, New Jersey	1
Commanding Officer, U.S. Army Electronics Research & Development Laboratory, Fort Monmouth, New Jersey, ATTN: SELRA/SL-ADT	1
Commanding Officer, U.S. Army Electronics Research & Development Laboratory, ATTN: SELRA/SL-ADJ (Responsible File & Record Unit) Fort Monmouth, New Jersey	1
Commanding Officer, U.S. Army Electronics Research & Development Laboratory, ATTN: SELRA/SL-TNR, Fort Monmouth, New Jersey	3
Commanding Officer, U.S. Army Electronics Research & Development Laboratory, ATTN: SELRA/SL-SMA, Fort Monmouth, New Jersey	7
OASD (R&E), Rm. 3E1065, The Pentagon, ATTN: Technical Library, Washington 25, D.C.	1
Office of the Chief Research & Development, Department of the Army, ATTN: CRD/M, Washington 25, D.C.	1
Commanding General, U.S. Army Electronics Command, ATTN: AMSEL, Fort Monmouth, New Jersey	1
Director, U.S. Naval Research Laboratory, ATTN: Code 2027, Washington 25, D. C.	1
Commanding Officer and Director, U.S. Navy Electronics Laboratory, San Diego 52, California	1
Commander, Air Force Command & Control Development Division, Air Research & Development Command, USAF, ATTN: CROTL Lawrence Hanscom Field, Bedford, Massachusetts	1

Address	No. of Copies
Commanding General, U.S. Army Electronic Proving Ground, ATTN: Technical Library, Fort Huachuca, Arizona	1
Commander, Armed Services Technical Information Agency, Arlington Hall Station, Arlington 12, Virginia, ATTN: TIPDR	10
Commander, Air Force Command & Control Development Division, Air Research & Development Command, USAF, ATTN: CRZC, Dr. M. R. Nagel, Lawrence Hanscom Field, Bedford, Massachusetts.	1
Chairman, U.S. Army Chemical Corps Meteorological Committee, Fort Detrick, Frederick, Maryland	1
Chief, Meteorology Division, U.S. Army Chemical Corps Proving Ground, Dugway Proving Ground, Utah	1
Chemical Research & Development Laboratories, Technical Library, Army Chemical Center, Edgewood, Maryland	1
Director, Atmospheric Sciences Programs, National Science Foundation, Washington 25, D.C.	1
Chief, Bureau of Naval Weapons (FAME), U.S. Navy Department, Washington 25, D.C.	1
Officer-in-Charge, Meteorological Curriculum, U.S. Naval Post Graduate School, Monterey, California	1
Chief of Naval Operations (OP 07), U.S. Navy Department, Washington 25, D.C.	1
Office of Naval Research, U.S. Navy Department, Washington 25, D.C.	1
U. S. Naval Research Laboratory (Code 7110), Washington 25, D.C.	1
Director, U.S. Naval Weather Service, U. S. Naval Station, Washington 25, D.C..	1
Officer-in-Charge, U.S. Naval Weather Research Facility, U.S. Naval Air Station, Bldg. R48, Norfolk, Virginia	1
U.S. Army Corps of Engineers, Waterways Experiment Station, P.O. Box 631, Vicksburg, Mississippi	1
Office of the Chief of Ordnance, Department of the Army, Washington 25, D.C.	1
Commanding Officer, U.S. Army Signal Missile Support Agency, White Sands Missile Range, New Mexico, ATTN: Missile Geophysics Div.	1

Address	No. of Copies
Office of Technical Services, Department of Commerce, Washington 25, D.C.	1
Library, National Bureau of Standards, Washington 25, D.C.	1
Director, National Weather Records Center, Arcade Building, ATTN: Mr. Fox, Asheville, North Carolina	1
Director, Federal Aviation Agency, ATTN: Mr. Hilsenrod, Pomona, N.J.	1
Signal Corps Liaison Office MIT, 77 Massachusetts Ave, Bldg 20C-116, ATTN: Mr. A. Bedrosian, Cambridge 39, Massachusetts	1
Library, U.S. Weather Bureau, Washington 25, D.C.	1
Climatic Center, U.S. Air Force, Annex 2, 225 D. Street S.E., Washington 25, D.C.	1
Director of Meteorology Research, Weather Bureau, Washington 25, D.C.	1
Mr. C. Gentry, National Hurricane Research Project, Aviation Bldg,. Room 517, 3240 N.W. 27th Avenue, Miami 42, Florida	1
Mr. R. Endlich, Stanford Research Institute, Menlo Park, California	1
The University of Texas, Electrical Engineering Research Laboratory, Austin, Texas, ATTN: Mr. Gerhardt	1
Department of Meteorology, University of Wisconsin, Madison, Wis.	1
Institute for Geophysics, University of California, Los Angeles, California, ATTN: Dr. C. Palmer	1
Department of Meteorology, University of Washington, Seattle, Washington, ATTN: Dr. Buettner	1
Department of Meteorology, Texas A&M College, College Station, Texas, ATTN: Dr. W. Clayton	1
Meteorology Department, Florida State University, Tallahassee, Florida, ATTN: Dr. La Seur	1
Meteorology Department, University of Chicago, Chicago, Illinois, ATTN: Dr. Fujita	1
University of Illinois, General Engineering Dept. 116 Transportation Bldg, ATTN: Dr. S. E. Pearson, Urbana, Illinois	1
Department of Meteorology and Oceanography, New York University, College of Engineering, University Heights, New York 53, New York	1

Address	No. of Copies
Meteorology Department, Pennsylvania State College, State College, Pennsylvania	1
Mr. H. Hiser, Radar Meteorology Section, University of Miami, Coral Gables, Florida	1
Dr. E. B. Kraus, Woods Hole Oceanographic Institute, Woods Hole, Massachusetts	1
Dr. A. Belmont, General Mills Electronics Group, 2003 E. Hennepin Ave., Minneapolis 13, Minnesota	1
Dr. H. Riehl, Department of Atmospheric Science, Colorado State University, Fort Collins, Colorado	1
Dr. W. Saucier, University of Oklahoma, Norman, Okla.	1
Dr. C. Ramage, Department of Meteorology and Oceanography, University of Hawaii, Honolulu 14, Hawaii	1
Department of Meteorology, Massachusetts Institute of Technology, Cambridge 39, Massachusetts	1